

**The effect of transition metal oxide dopants on the structure, morphology, surface texture and catalytic properties of FeMgO nanomaterials towards dehydrogenation and aldol condensation reactions**

**Sahar A. El-Molla\*, Hala R. Mahmoud**

*Department of Chemistry, Faculty of Education, Ain Shams University, Roxy 11757, Cairo, Egypt*

\* Corresponding author , E-mail address :sahar[elmolla@yahoo.com](mailto:saharelmolla@yahoo.com)

**ABSTRACT**

The impregnation method was successfully used to prepare FeMgO and transition metal ( $\text{Cu}^{2+}$ ,  $\text{Cr}^{3+}$ ) -doped FeMgO nanomaterials calcined at 500 and 700 °C. The as-prepared catalysts were characterized by X-ray diffraction (XRD), high-resolution transmission electron microscopy (HR-TEM), energy dispersive spectroscopic (EDS), specific surface areas ( $S_{\text{BET}}$ ) and catalytic conversion of 2-propanol at 225-400 °C. The results showed presence of MgO spherical nanoparticles as aggregates of uniform trigonal shapes in the catalyst calcined at 500 °C. Doping with  $\text{Cu}^{2+}$  ions modified the morphology to much dispersed spherical iron oxide nanoparticles while doping with  $\text{Cr}^{3+}$  species increased the agglomeration of the obtained nanoparticles. Doping FeMgO nanomaterials with  $\text{Cu}^{2+}$  ions brought about a measurable increase in its  $S_{\text{BET}}$ , opposite result was found in case of doping with  $\text{Cr}^{3+}$  ions. Pure and  $\text{Cu}^{2+}$ -doped nanomaterials act as active dehydrogenation catalysts yielding acetone. CuFeMgO system was highly selective to methyl isobutyl ketone (MIBK). CrFeMgO system was highly selective to propene. The catalytic activity and selectivity of the investigated catalysts depend on both of calcination temperature, reaction temperature, and the nature dopant.

**Keywords:** Nanomaterials; Doping;  $\text{Fe}_2\text{O}_3/\text{MgO}$ ; 2-propanol conversion; Catalysis

## 1. Introduction

Nanomaterials with average grain sizes ranging from 1 to 100 nm exhibit properties that were often rather different relative to those of bulk counterparts [1, 2]. The electronic, magnetic, optical and catalytic properties of these materials have been found to be different from those of bulk counterparts and to depend sensitively on size, morphology and composition [3]. In particular, nano-sized iron oxide-based catalysts are very important catalysts in oxidation processes [4]. Despite its catalytic potential and its availability,  $\alpha$ - $\text{Fe}_2\text{O}_3$  has a low thermal stability to sintering, which is accompanied by deactivation [5]. Therefore, supporting iron oxide usually results in modification of its textural, structural, and catalytic properties [4]. It is known that the activity and selectivity of a large variety of catalysts can be modified by loading them on a fine support and doping them with certain foreign oxides [6].

Magnesium oxide (MgO) is a versatile metal oxide having numerous applications in many fields. It has been used as a catalyst and catalyst support for various organic reactions [7,8], as an antimicrobial material [9], and electrochemical biosensor [10]. Formation of MgO nanostructures with a small crystallite size of less than 100 nm and homogeneous morphology has attracted much attention due to their unique physicochemical properties including high surface area-to-volume ratio. It is widely accepted that the properties of MgO nanostructures depend strongly on the synthesis methods and the processing conditions [4,11].

It has been reported that  $\text{Fe}_2\text{O}_3/\text{MgO}$  nano-composite prepared by impregnation, co-precipitation and hydrothermal have biomedical, catalytic and magnetic applications [4,11]. It was reported that doping the catalytic system with certain foreign oxides is accompanied by significant modifications in its thermal stability, surface, and catalytic properties [6]. It has been reported that doping the magnetite with chromium ions has a remarkable effect on its crystallinity, surface area, porosity and magnetic properties. Presence chromium ions strongly increased the catalytic activity towards Fenton reaction [12]. Doping magnetite with chromium species restricted its rapid thermal sintering, thereby enhanced the WGS activity of the Fe/Cr catalyst [13]. Cr-doped  $\text{Fe}_2\text{O}_3$  are known as an active catalyst for sulfuric acid decomposition without showing any visible deactivation [14].

It has been reported that copper ions addition to iron oxide improved  $\text{Fe}^{3+}$  species reducibility into  $\text{Fe}^{2+}$ , which promotes the WGS activity [13]. It was reported that doping catalyst with Cu-species increases the lattice oxygen mobility and concentration of surface hydroxyl groups which results in better catalytic activity [13]. The supported copper–iron system has been studied in CO oxidation at low temperature [15]. Deposition metal cations as  $\text{Ni}^{2+}$ ,  $\text{Fe}^{3+}$ ,  $\text{Cu}^{2+}$  and  $\text{Cr}^{3+}$  species on MgO producing new centers with different acid–base properties have been reported [16, 17]. Conversion of 2-propanol on metal oxides surface has been employed frequently as a probe of surface acid-base properties [18, 19]. The detected products of 2-propanol conversion were propene, acetone and MIBK (methyl isobutyl ketone) [16]. MIBK was produced by using bifunctional catalyst such as  $\text{CuM}_I\text{M}_{II}\text{O}_x$  where  $\text{M}_I$ ,  $\text{M}_{II}$  are metal cations such as  $\text{Mg}^{2+}$ ,  $\text{Al}^{3+}$  or  $\text{Ce}^{3+}$  in one step [20].

The aim of this work is studying the effect of the copper and chromium oxides doping on  $\text{Fe}_2\text{O}_3/\text{MgO}$  nanomaterials for 2-propanol conversion. Furthermore, the as-prepared pure and doped FeMgO nanomaterials were characterized by X-ray diffraction (XRD), high-resolution transmission electron microscopy (HR-TEM), energy dispersive spectroscopic (EDS) and specific surface areas ( $S_{\text{BET}}$ ). The 2-propanol conversion of pure and doped FeMgO nanomaterials was investigated.

## 2. Experimental

### 2.1. Materials

All reagents were of analytical grade and they were purchased and used as received without further purification: magnesium carbonate ( $\text{MgCO}_3$ , Oxford), iron nitrate nonahydrate ( $\text{Fe}(\text{NO}_3)_3 \cdot 9\text{H}_2\text{O}$ , Oxford), Chromium (III) nitrate nonahydrate ( $\text{Cr}(\text{NO}_3)_3 \cdot 9\text{H}_2\text{O}$ , Oxford), copper nitrate trihydrate ( $\text{Cu}(\text{NO}_3)_2 \cdot 3\text{H}_2\text{O}$ , Oxford), ammonia solution ( $\text{NH}_4\text{OH}$ , Alpha) and iso-propanol (absolute) (for HPLC,  $\geq 99\%$ ). Bi-distilled water was used for the preparation of all the catalysts.

### 2.2. Catalyst preparation

0.1 $\text{Fe}_2\text{O}_3$ -MgO catalyst was prepared by impregnation method using a known amount  $\text{MgCO}_3$  with a known amount of iron nitrate dissolved in the least amount of bi-distilled water necessary to make a paste.

The resulting paste was dried at 110 °C and then calcined at 500 and 700 °C for 3 h. This sample was nominated as FeMgO. Fe<sub>2</sub>O<sub>3</sub> mass content (wt %) in these samples was fixed at 9.1 %.

The CuO and Cr<sub>2</sub>O<sub>3</sub>/Fe<sub>2</sub>O<sub>3</sub>-MgO nanomaterials were prepared using a known mass of MgCO<sub>3</sub> impregnated with solutions containing a constant amount of iron nitrate and different proportions of copper nitrate or chromium nitrates, followed by drying at 110 °C for 8 h. Finally, the as-prepared nanomaterials were calcined at 500 and 700 °C for 3h. The molar ratio of CuO and Cr<sub>2</sub>O<sub>3</sub> added were 0.5, 1.0 and 2.0 mol %. The formula x-CuFeMgO or x-CrFeMg will be used throughout the paper to represent the different composites where x refers to the molar % dopant content.

### 2.3. Catalyst characterization

X-ray diffraction powder patterns were recorded at room temperature on a Bruker AxSD8 Advance X-ray diffractometer (Germany), using the Bragg-Brentano configuration and the CuK $\alpha$ , radiation  $\lambda=1.5404$  Å. The morphology of the catalysts was observed by high-resolution transmission electron microscopy (HR-TEM) equipped with energy dispersive spectroscopic (EDS) microanalysis system (JEM-2100CX (JEOL)). The surface areas of the prepared catalysts were obtained using nitrogen gas adsorption at -196 °C on a Quantachrome NOVA 2000 automated gas-sorption apparatus model 7.11 (USA). Before each N<sub>2</sub> sorption measurement, samples were degassed at 200 °C for 2 h.

### 2.4. Catalytic activity test

Catalytic activity tests of the prepared catalysts were determined by using iso-propanol conversion reaction at different temperatures varying between 225 to 400 °C, the catalytic reaction was conducted in a flow reactor under atmospheric pressure. Thus, a 50 mg catalyst sample was held between two glass wool plugs in a 20 cm long Pyrex glass reactor tube with 1 cm internal diameter, packed with quartz fragments of 2–3 mm length. The temperature of the catalyst bed was regulated and controlled to within  $\pm 1$ °C. Argon gas was used as a diluent and a carrier gas for 2-propanol vapor, which was introduced into the reactor through an evaporator/saturator containing the liquid reactant at constant temperature 35 °C. The flow rate of the carrier gas (argon) was maintained at 30 ml/min. Before carrying out catalytic activity measurements, each catalyst sample was activated by heating at 350 °C in a current of argon for 1 h and then cooled to the

catalytic reaction temperature. The reaction products in the produced gaseous phases were analyzed chromatographically using a Perkin-Elmer Auto System XL gas chromatograph fitted with a flame ionization detector. The column used was a fused silica glass capillary column type PE-CW length 15 m-1.0  $\mu\text{m}$  of Perkin-Elmer.

### 3. Results and discussion

#### 3.1. Effect of $\text{Cr}^{3+}$ and $\text{Cu}^{2+}$ ions doping on the structural and morphological characteristics of

##### FeMgO nanomaterial

XRD is used for identification of the crystal phase and crystallite size of each phase present. XRD patterns of FeMgO, 1%CrFeMgO, 1%CuFeMgO and 2%CuFeMgO catalysts calcined at 500 and 700  $^{\circ}\text{C}$  were shown in Fig. 1. The effect of CuO and  $\text{Cr}_2\text{O}_3$  doping on the degree of ordering and crystallite size of MgO phase was investigated as shown in Table 1. XRD of pure and doped nanomaterials calcined at 500  $^{\circ}\text{C}$  (not shown) contains diffraction lines at d-spacing = 2.43, 2.11, 1.49, 1.27 and 1.216  $\text{\AA}$  due to MgO phase (periclase) (JCPDS 4-829) with moderate degree of ordering. There is no diffraction lines related to  $\text{Fe}_2\text{O}_3$ ,  $\text{MgFe}_2\text{O}_4$  phase or copper and chromium species in the doped catalysts, implying that the previous phases exist in a highly dispersed state on MgO surface with small size to be detected by X-ray powder diffractometer [21]. So, nanocrystalline magnesium oxide (17.5 nm) acted as a convenient support for hematite. Doping FeMgO system calcined at 500  $^{\circ}\text{C}$  with CuO or  $\text{Cr}_2\text{O}_3$  decreased both of the degree of ordering and crystallite size of MgO phase, this could be due to a possible coating of the MgO crystallite with dopant oxides films which hinders the particle adhesion process, thus limiting their grain growth during the course of heat treatment [22]. The computed lattice parameter (a) of MgO phase in FeMgO and 1%CuFeMgO nanomaterials calcined at 500  $^{\circ}\text{C}$  is bigger than the standard value. While chromia-doping decreases the lattice parameter (a) value of MgO phase. The possible dissolution of big sized cations as  $\text{Fe}^{2+}$  (0.76  $\text{\AA}$ ), and  $\text{Cu}^{2+}$  (0.72  $\text{\AA}$ ) or small sized cations as  $\text{Cr}^{3+}$  (0.44  $\text{\AA}$ ) in MgO lattice can explain the obtained results [23, 24]. The close ionic radii of the dopants species to that of  $\text{Mg}^{2+}$  (0.66  $\text{\AA}$ ) enable it to enter the lattice, causing a change in the inter-planar distance. It has been reported that the semi-diameters of  $\text{Mg}^{2+}$ ,  $\text{Fe}^{3+}$ , and  $\text{Fe}^{2+}$  are 0.66, 0.64 and 0.76  $\text{\AA}$ , respectively [23, 24], So,  $\text{Fe}^{3+}$  could easily get into the crystal

lattice instead of  $\text{Mg}^{2+}$  due to their close semi-diameters. But the size of  $\text{Fe}^{2+}$  is much bigger than  $\text{Mg}^{2+}$  so that it is hard to be incorporated into the lattice. The observed shift in MgO lattice parameter to lower value due to Cr- addition was explained by Vegard's law [25], which showed dependence the lattice parameter on Mg-Cr-O system composition, that behave as a solid solution [26]. It has been reported that there is a solid-solid interaction between chromium species and magnesia yielding magnesium chromate or chromite depending on calcination temperature [17].

Increasing the calcination temperature of pure and doped nanomaterials from 500 to 700 °C increased the degree of ordering and crystallite size of MgO phase. New diffraction lines due to  $\text{MgFe}_2\text{O}_4$  phase were observed. Doping FeMgO catalyst with copper and chromium oxides (1 mol %) calcined at 700 °C resulted in a decrease in both of crystallite size and degree of ordering of MgO and  $\text{MgFe}_2\text{O}_4$  phases, increasing the  $\text{Cu}^{2+}$ -species content to 2% resulted in an opposite behavior. The observed increase in the crystallite sizes of MgO and  $\text{MgFe}_2\text{O}_4$  phases for pure and doped solids due to increasing the calcination temperature from 500 to 700 °C could be explained in the light of the grain growth mechanism or sintering processes [27] and/or the solid-solid interaction between  $\text{Fe}_2\text{O}_3$  and MgO yielding  $\text{MgFe}_2\text{O}_4$  which enhanced by 2% CuO-doping.

Fig. 2 shows the HR-TEM images of FeMgO, 1%CrFeMgO and 2%CuFeMgO catalysts calcined at 500 °C. The aggregates of uniform trigonal shapes and spherical nanoparticles with average diameter 25 nm were observed in FeMgO nanomaterial. Furthermore, the 1%CrFeMgO catalyst possesses very small aggregate uniform spherical nanoparticles with average diameter 9 nm. Similarly, a small aggregate uniform spherical nanoparticles with average diameter 6 nm was obtained for the 2%CuFeMgO nanoparticle. Furthermore, it has been possible to detect very small darker spots highly dispersed in the oxide layer. These spots correspond to very small iron oxide particles completely dispersed [4]. The average particle size calculated from the TEM micrographs is consistent with the average crystallite size obtained from XRD measurement. To investigate the elemental composition of FeMgO and 1%CrFeMgO catalysts, energy dispersive spectroscopy (EDS) analysis was carried out. The EDS results of the prepared nanomaterials prove the presence of iron, magnesium, chromium and oxygen elements as shown in Fig. 3. The analytical results from EDS are virtually identical or very close to the nominal wt% of FeMgO and 1%CrFeMgO catalysts. The

observed crystallographic and morphological changes in FeMgO system as a result of copper or chromium oxides-doping are expected to induce changes in its surface and catalytic properties.

### 3.2. Specific surface areas

The specific surface areas ( $S_{\text{BET}}$ ) of the prepared nanomaterials calcined at 500 and 700 °C were determined from nitrogen adsorption isotherms conducted at -196 °C and the data were listed in the last column in Table 1.  $S_{\text{BET}}$  of the FeMgO catalyst calcined at 500 °C increased by  $\text{Cu}^{2+}$ -doping. Opposite behavior was observed in chromia doping. The observed increase in the  $S_{\text{BET}}$  of FeMgO system due to  $\text{Cu}^{2+}$ -doping might be due to (i) creation of a big deal of pores created from libration of nitrogen oxides gases in the course of the thermal decomposition of copper nitrate dopant. (ii) Fine dispersion of CuO particles on the surface of FeMgO system due to decreasing the degree of ordering of MgO phase as shown in XRD section. The observed decrease in the  $S_{\text{BET}}$  of FeMgO system calcined at 500 °C due to  $\text{Cr}^{3+}$ -doping could be discussed in terms of (i) possible blocking of some pores by dopant cation also, (ii) possible solid-solid interactions between chromia and the support [17]. The rise in the calcination temperature of the pure and doped FeMgO samples from 500 to 700 °C brought about a significant decrease in their  $S_{\text{BET}}$ . This observed decrease could be due to increasing the degree of ordering and the crystallite sizes of the detected phases. The observed changes in the textural properties of the FeMgO solids as a result of copper and chromium species doping and increasing the calcination temperature should modify the concentration of catalytically active constituents taking part in the catalyzed reaction.

### 3.3. Catalytic conversion of 2-propanol in presence of pure and doped FeMgO nanomaterials

The catalytic conversion of 2-propanol was carried out over pure and variously doped FeMgO catalysts calcined at 500 and 700 °C. The change in the percentage conversion as a function of reaction temperature varied between 225 and 400 °C was investigated. Table 2 shows the activity and selectivity of the investigated catalysts toward the products of 2-propanol conversion in the gas phase. Fig. 4 depicts the total iso-propanol conversion of pure and doped FeMgO catalysts calcined at 700 °C as a function of the reaction temperature. The main reaction promoted by these catalysts was dehydrogenation of 2-propanol to the carbonyl derivative (acetone) and dehydration to the corresponding alkenes (propene). Inspection of Table 2

and Fig. 4: (i) the activities of pure and doped-FeMgO catalysts increased with increasing reaction temperature in all instances. (ii) Catalytic activity of pure and doped-FeMgO catalysts calcined at 500°C is higher than that calcined 700°C. The catalytic activity of FeMgO toward 2-propanol conversion to yield acetone is due to nano-iron oxide supported on magnesia. It has been reported that iron oxide nanomaterial is novel and promising catalyst for industrial applications in selective oxidations [28-30]. (iii) Doping FeMgO catalysts calcined at 500°C, with copper or chromium ions increased its catalytic activity and the catalytic activity of the CrFeMgO solids is lower than that of CuFeMgO. (iv) The catalytic activity of CrFeMgO samples is much lower than that of FeMgO solid calcined at 700 °C. (v) Doping FeMgO with increasing amounts of Cu<sup>2+</sup> species increased the selectivity towards dehydrogenation process yielding acetone. Doping with 1 and 2 % Cu<sup>2+</sup> followed by calcination at 500 °C yielded condensation product (MIBK). Dehydrogenation reaction is carried out on basic sites to yield acetone as main product [16, 31]; however, the reaction temperature as well as partial pressure of IPA also influences strongly on conversion [32, 33]. MIBK is produced in novel one-step synthesis from 2-propanol at low temperature and atmospheric pressure [16, 31]. So, the observed increase in the catalytic activity and dehydrogenation selectivity of FeMgO as a result of Cu<sup>2+</sup>-doping may be due to an effective increase in the degree of dispersion of iron oxide through decreasing both of the degree of ordering and crystallite size of MgO phase as support material (*c.f.* Table 1). Possible synergism between CuO and MgO play another factor [16, 31]. An important factor one cannot overlook is the modification of FeMgO morphology as a result of doping with Cu<sup>2+</sup> species (*see characterization section*) to more dispersed spherical iron oxide nanoparticles while doping with Cr<sup>3+</sup> species increased the agglomeration of the obtained nanoparticles. This was reflected on surface area and catalytic activity of the doped FeMgO system. The active sites needed for dehydrogenation are copper oxide species beside presence of nanosized Fe<sup>3+</sup> ions and medium-strength basic active sites [Mg(M)-O] with high density [34]. The concentration of the active sites contributed in formation of acetone or condensation products is big at low calcination temperature, low reaction temperature. (vi) CrFeMgO samples exhibit high selectivity to propene in all reaction temperatures. The higher selectivity to dehydration process (yielding propene) in case of CrFeMgO samples may be due to increasing the acidic active site numbers on the catalysts surface [35]. The dehydration reaction is carried out through 2-propanol adsorption onto Brønsted or Lewis acid sites followed by the scission of hydroxyl group to form alkoxy species. In the presence of Lewis acid sites, the



hydroxyl group cleaved in the first step and the proton generated is combined again and desorbed as water, thus regenerating the Lewis acid site. So, increasing the selectivity towards propene formation as a result of Cr<sub>2</sub>O<sub>3</sub>-doping is owing to increasing surface hydroxyl groups and /or Cr<sup>3+</sup> species (acidic centers).

The observed decrease in the catalytic activity and selectivity due to increasing the calcination temperature of the various investigated catalysts from 500 to 700°C could be attributed to the effective increase in the crystallite size and degree of crystallinity of the MgO-support phase and decrease of the surface areas of the investigated samples as shown in Table 1. Also the possible decrease in the surface concentrations of the supported transition metal ions could play an important role. It has been reported that increasing the calcination temperature of MgO-based solids decreases the concentration of magnesium defect per unit lattice cell (cationic defects which are responsible for its basic sites) [36]. So, presence ferrite species as shown in XRD-section may play an important role in decreasing the catalytic activity and selectivity of the pure and doped catalysts calcined at 700 °C. The observed decrease in the catalytic activity of CrFeMgO calcined at 700 °C with comparison to FeMgO sample may be due to possible formation of chromite species [17]. The chromite species are known as hydrogenation catalysts such as copper chromite CuCr<sub>2</sub>O<sub>4</sub> in hydrogenation of acetone to 2-propanol. So, the possible obtained chromite may shift the reaction towards formation 2-propanol [37].

In conclusion, the catalytic activity and selectivity of the investigated solids depend on each of calcination temperature, reaction temperature, and the nature of foreign cation-doping.

#### 4. Conclusions

In summary, pure and Cu<sup>2+</sup> or Cr<sup>3+</sup> - doped FeMgO nanomaterials were successfully prepared by impregnation method. The Cu<sup>2+</sup> and Cr<sup>3+</sup> - doped FeMgO nanomaterials showed significantly modified structural and morphological characteristics as compared with the un-doped FeMgO catalyst. The Cu<sup>2+</sup> - doped FeMgO nanomaterial increased its S<sub>BET</sub>. It was observed that the Cu<sup>2+</sup> or Cr<sup>3+</sup> -doping much increased the catalytic activity of FeMgO nanomaterial in 2-propanol conversion to an extent proportional to the amount of dopant added. Pure and Cu<sup>2+</sup> doped catalysts acted as active dehydrogenation catalysts yielding acetone. Cu<sup>2+</sup>-doped catalysts enhanced formation MIBK. Cr<sup>3+</sup>-doping enhanced formation of propene. The

catalytic activity and selectivity of FeMgO nanomaterial depend on each of calcination temperature, reaction temperature, and the nature of foreign cation added as a dopant.

## References

- [1] P. Hajra, P. Brahma, S. Dutta, S. Banerjee, D. Chakravorty, Enhancement of magnetic anisotropy in mechanically attrited Cr<sub>2</sub>O<sub>3</sub> nanoparticles, *J. Magn. Magn. Mater.* 324 (2012) 1425–1430.
- [2] N.C.S. Selvam, A. Manikandan, L.J. Kennedy, J.J. Vijaya, Comparative investigation of zirconium oxide (ZrO<sub>2</sub>) nano and microstructures for structural, optical and photocatalytic properties, *J. Colloid Interface Sci.* 389 (2013) 91–98.
- [3] S.A. Makhlof, Z.H. Bakr, H. Al-Atta, M.S. Moustafa, Structural, morphological and electrical properties of Cr<sub>2</sub>O<sub>3</sub> nanoparticles, *Mater. Sci. Eng. B* 178 (2013) 337–343.
- [4] S.A. El-Molla, H.R. Mahmoud, Synthesis, textural and catalytic properties of nanosized Fe<sub>2</sub>O<sub>3</sub>/MgO system, *Mater. Res. Bull.* 48 (2013) 4105–4111.
- [5] X. Liu, K. Shen, Y. Wang, Y. Wang, Y. Guo, Y. Guo, Z. Yong, G. Lu, Preparation and catalytic properties of Pt supported Fe-Cr mixed oxide catalysts in the aqueous phase reforming of ethylene glycol, *Catal. Commun.* 9 (2008) 2316–2318.
- [6] S.A. El-Molla, L.I. Ali, N.H. Amin, A.A. Ebrahim, H.R. Mahmoud, Effect of Ag-doping of nanosized FeMgO system on its structural, surface, spectral, and catalytic properties, *Chem. Papers* 66 (2012) 8) 722–732.
- [7] R. Sathyamoorthy, K. Mageshwari, S.S. Mali, S. Priyadarshini, P.S. Patil, Effect of organic

capping agent on the photocatalytic activity of MgO nanoflakes obtained by thermal decomposition route, *Ceram. Int.* 39 (2013) 323–330.

- [8] G. Yuan, J. Zheng, C. Lin, X. Chang, H. Jiang, Electrosynthesis and catalytic properties of magnesium oxide nanocrystals with porous structures, *Mater. Chem. Phys.* 130 (2011) 387–391.
- [9] K. Zhang, Y. An, L. Zhang, Q. Dong, Preparation of controlled nano-MgO and investigation of its bactericidal properties, *Chemosphere* 89 (2012) 1414–1418.
- [10] A. Umar, M.M. Rahman, Y.-B. Hahn, MgO polyhedral nanocages and nanocrystals based glucose Biosensor, *Electrochem. Commun.* 11 (2009) 1353–1357.
- [11] S.A. El-Molla, G.A. Fagal, N.A. Hassan, G.M. Mohamed, Effect of the method of preparation on the physicochemical and catalytic properties of nanosized Fe<sub>2</sub>O<sub>3</sub>/MgO, *Res. Chem. Intermed.* 39 (2013) 1–11.
- [12] F. Magalhaês, M.C. Pereira, S.E.C. Botrel, J.D. Fabris, W.A. Macedo, R. Mendonça, R.M. Lago, L.C.A. Oliveira. Cr-containing magnetites Fe<sub>3-x</sub>Cr<sub>x</sub>O<sub>4</sub>: The role of Cr<sup>3+</sup> and Fe<sup>2+</sup> on the stability and reactivity towards H<sub>2</sub>O<sub>2</sub> reactions, *Appl. Catal. A* 332 (2007) 115–123.
- [13] A. Khan, P.G. Smirniotis, Relationship between temperature-programmed reduction profile and activity of modified ferrite-based catalysts for WGS reaction, *J. Mol. Catal. A* 280 (2008) 43–51.
- [14] A. M. Banerjee, A.R. Shirole, M.R. Pai, A.K. Tripathi, S.R. Bharadwaj, D. Das, P.K. Sinha. Catalytic activities of Fe<sub>2</sub>O<sub>3</sub> and chromium doped Fe<sub>2</sub>O<sub>3</sub> for sulfuric acid

decomposition reaction in an integrated boiler, preheater, and catalytic decomposer,

Appl. Catal. B 127 (2012) 36-46.

[15] T. Cheng, Z. Fang, Q. Hu, K. Han, X. Yang, Y. Zhang, Low-temperature CO oxidation over CuO/Fe<sub>2</sub>O<sub>3</sub> catalysts Catal. Commun. 8 (2007) 1167–1171.

[16] S.A. El-Molla, Dehydrogenation and condensation in catalytic conversion of *iso*-propanol over CuO/MgO system doped with Li<sub>2</sub>O and ZrO<sub>2</sub>, Appl. Catal. A 298 (2006) 103–108.

[17] S.A. El-Molla, Surface and catalytic properties of Cr<sub>2</sub>O<sub>3</sub>/MgO system doped with manganese and cobalt oxides, Appl. Catal. A 280 (2005) 189-197.

[18] J.E. Rekoske, M.A. Barteau, Kinetics and Selectivity of 2-Propanol Conversion on Oxidized Anatase TiO<sub>2</sub>, J. Catal. 165 (1997) 57-72.

[19] A. Gervasini, A. Auroux, Acidity and basicity of metal oxide surfaces II. Determination by catalytic decomposition of isopropanol J. Catal. 131 (1991) 190-198.

[20] J.I. Dicosimo, G. Torres, C.R. Apesteguia, One-Step MIBK Synthesis: A New Process from 2-Propanol, J. Catal. 208 (2002) 114-123.

[21] T. Tsoncheva, J. Roggenbuck, M. Tiemann, L. Ivanova, D. Paneva, I. Mitov, C. Minchev, Iron oxide nanoparticles supported on mesoporous MgO and CeO<sub>2</sub>: A comparative physicochemical and catalytic study, Micropor. Mesopor. Mater. 110 (2008) 339-346.

[22] N.R.E. Radwan, Influence of La<sub>2</sub>O<sub>3</sub> and ZrO<sub>2</sub> as promoters on surface and catalytic properties of CuO/MgO system prepared by sol–gel method, Appl. Catal. A 299 (2006) 103–121.

- [23] R.C. Weast, Handbook of chemistry and physics (1984). (65<sup>th</sup> ed., pp. 165). Boca Raton, FL, USA: CRC Press.
- [24] G.A. El-Shobaky, A.A. Mostafa, Solid–solid interactions in Fe<sub>2</sub>O<sub>3</sub>/MgO system doped with aluminium and zinc oxides, *Thermochim. Acta*, 408 (2003) 75–84.
- [25] M. Saraiva, V. Georgieva, S. Mahieu, K. Van Aeken, A. Bogaerts, D. Depla, Compositional effects on the growth of Mg(M)O films, *J. Appl. Phys.* 107 (2010) 034902 – 034902-10.
- [26] S. Vyas, R.W. Grimes, D.J. Binks, F. Rey, Metastable solid solutions of alumina in magnesia, *J. Phys. Chem. Solids* 58 (1997) 1619-1624.
- [27] W.M. Shaheen, Thermal solid–solid interaction and catalytic properties of CuO/Al<sub>2</sub>O<sub>3</sub> system treated with ZnO and MoO<sub>3</sub>, *Thermochim. Acta*, 385 (2002)105–116.
- [28] J. Ge, T. Huynh, Y. Hu, Y. Yin, Hierarchical Magnetite/Silica Nanoassemblies as Magnetically Recoverable Catalyst–Supports, *Nano Lett.* 8 (2008) 931-934.
- [29] A.C. Silva, D.Q.L. Oliveira, L.C.A. Oliveira, T.C. Ramalho, Nb-containing hematites Fe<sub>2-x</sub>Nb<sub>x</sub>O<sub>3</sub>: The role of Nb<sup>5+</sup> on the reactivity in presence of the H<sub>2</sub>O<sub>2</sub> or ultraviolet light, *Appl. Catal. A* 357 (2009)79–84.
- [30] L.C.A. Oliveira, F. Zaera, I. Lee, D.Q. Lima, T.C. Ramalho, A. Silva, E. M.B. Fonseca, Nb-doped hematites for decomposition of isopropanol: Evidence of surface reactivity by *in situ* CO adsorption, *Appl. Catal. A*. 368 (2009) 17–21.
- [31] S.A. El-Molla, G. A. El-Shobaky, N.H. Amin, M.N. Hammed, S.N. Sultan, Catalytic properties of Pure and K<sup>+</sup>- Doped CuO/MgO System towards 2-Propanol Conversion, *J.*

- Mex. Chem. Soc. 57(2013)1-7.
- [32] E. Ortiz-Islas, T. Lopez, J. Navarrete, X. Bokhimi, R. Gomez, High selectivity to isopropyl ether over sulfated titania in the isopropanol decomposition, *J. Mol. Catal. A* 228 (2005) 345–350.
- [33] F. Trejo, M. S. Rana, J. Ancheyta, A. Rueda, Hydrotreating catalysts on different supports and its acid–base properties, *Fuel* 100 (2012) 163–172
- [34] G. Torres, C.R. Apesteguia, J.I. Di Cosimo, One-step methyl isobutyl ketone (MIBK) synthesis from 2-propanol: Catalyst and reaction condition optimization, *Appl. Catal. A* 317(2007) 161-170.
- [35] M. Sadiq, M. Bensitel, K. Nohair, J. Leglise, C. Lamonier, Effect of calcination temperature on the structure of vanadium phosphorus oxide materials and their catalytic activity in the decomposition of 2-propanol, *J. of Saudi Chem. Soc.* 16 (2012) 445–449.
- [36] J.A. Wang, X. Bokhimi, O. Novaro, T. López, R. Gómez, Effects of the surface structure and experimental parameters on the isopropanol decomposition catalyzed with sol–gel MgO, *J. Mol. Catal. A* 145 (1999) 291–300.
- [37] T.M. Yurieva, L.M. Plyasova, O.V. Makarova, T.A. Krieger. Mechanisms for hydrogenation of acetone to isopropanol and of carbon oxides to methanol over copper-containing oxide catalysts, *J. Mol. Catal. A* 113 (1996) 455-468.

### Figures captions

**Fig. 1.** XRD of the pure and doped catalysts with  $\text{Cu}^{2+}$ - and  $\text{Cr}^{3+}$ -species calcined at 700 °C. (A) Pure FeMgO, (B) 1% CrFeMgO, (C) 1% CuFeMgO, (D) 2% CuFeMgO. Lines (1) refer to

MgO and lines (2) refer to  $\text{MgFe}_2\text{O}_4$  phases.

**Fig. 2.** HR-TEM images of FeMgO, 1%CrFeMgO and 2%CuFeMgO catalysts calcined at 500 °C.

**Fig. 3.** EDS analysis of FeMgO and 1%CrFeMgO catalysts calcined at 500 °C.

**Fig.4.** Total conversion of 2-propanol as a function of reaction temperature over pure and variously

$\text{Cu}^{2+}$ - and  $\text{Cr}^{3+}$ -doped FeMgO catalysts calcined at 700 °C.

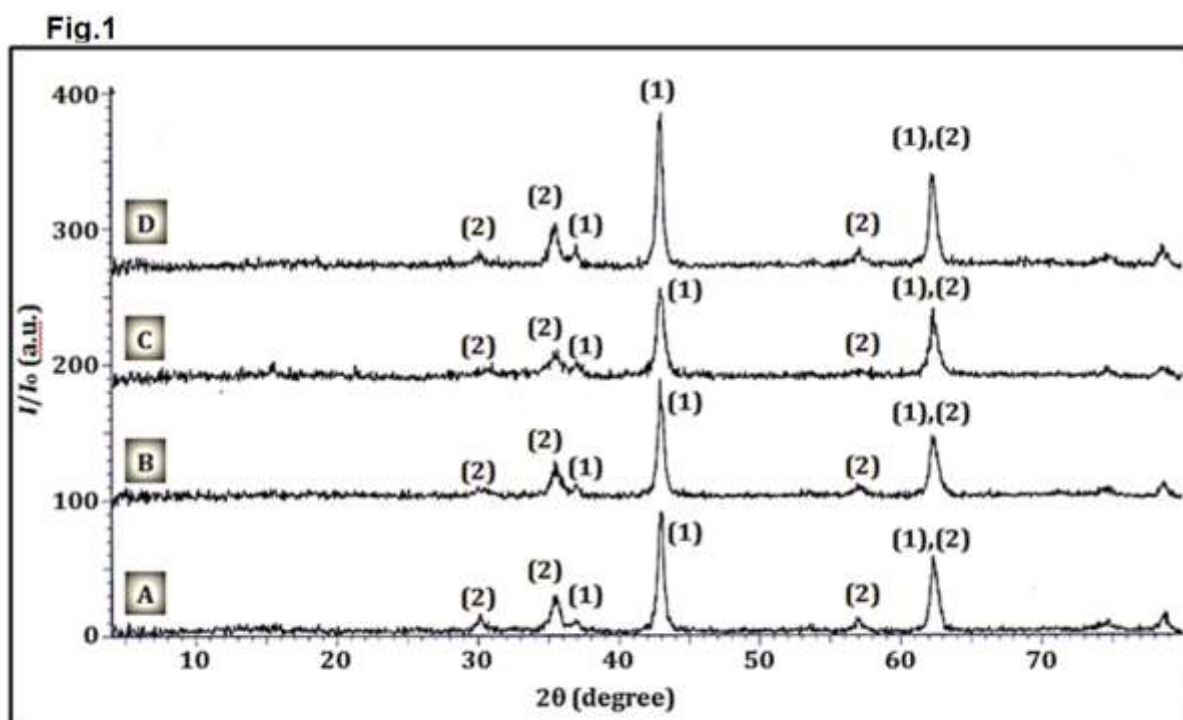


**Fig.2**

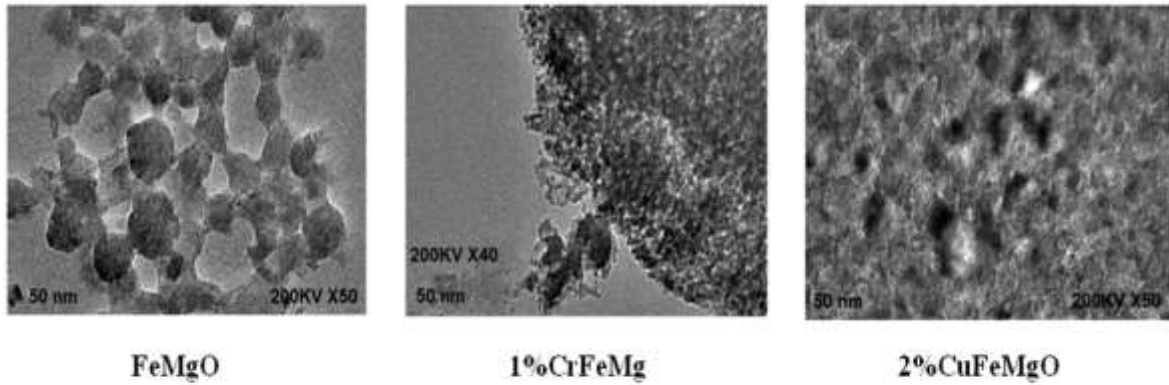
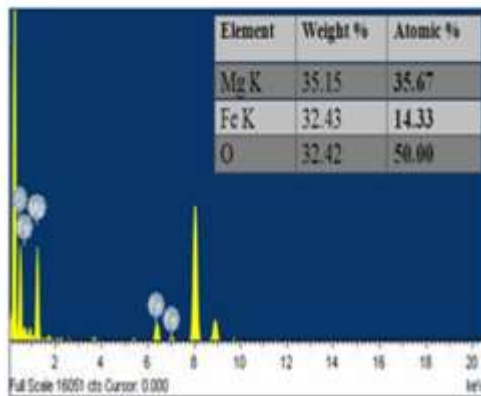
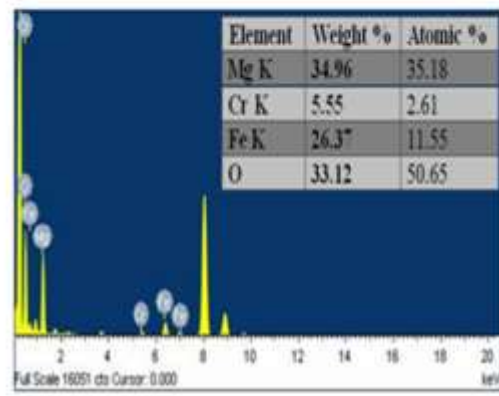


**Fig.3**



**FeMgO**



**1%CrFeMg**



Fig.4

